Performance Characteristics of a Reflector Ultra Wideband Impulse Radiating Antenna

Sidhartha Ghosh[1], B K Sarkar[2], S V Pandey[3]
[1,3]Dept. of Electronics & Electrical Communication Engineering
Indian Institute of Technology, Kharagpur – 721 302
[2] ISRO Chair Professor, Indian Institute of Technology, Kharagpur – 721 302
sghosh@ece.iitkgp.ernet.in

***Abstract**:*

In this paper, CST-MS was used to model and simulate an Ultra wideband Impulse radiating antenna using high voltage feeding mechanism. Model views are shown and the results of frequency domain simulation up to 7 GHz are plotted for the UWB Impulse Radiating antenna. The feed and the IRA were simulated for various characteristics like frequency domain reflections, VSWR, insertion loss, radiation pattern and gain etc. The half power beamwidth and antenna factor of the antenna were also calculated. The antenna is wideband, non dispersive, directive and has low VSWR. The basic concepts of IRA are reviewed. The reflector IRA was designed, analyzed and simulated in CST-MS. The near-field and far-field characteristics of the reflector IRA are studied using the frequency domain results.

***Key Words:** Coplanar Conical Transmission line, Paraboloidal reflector antenna, Simultaneous feed.*

I. Introduction

The radiation of a short electromagnetic pulse is useful in a variety of applications, such as non-destructive testing, ultra-wide band weapons, and remote sensing. In remote sensing applications, short-pulse radiation is used to locate and identify targets. Typically, a short pulse is sent in the direction of a target, and the temporal information in the reflected signal is used to distinguish the target from other objects in the vicinity. In order to radiate a short pulse, the antenna must be both non-dispersive and capable of radiating over a broad bandwidth. Some broadband antennas suffer from severe dispersion. For remote sensing applications, dispersion is an undesired characteristic because it will cause the signal from a target to be spread out in time making it more difficult to distinguish the target. Impulse-radiating antennas (IRAs) are the antennas that can transmit and receive short pulses. The IRA is an equi-phase aperture that is fed by a spherical transverse electromagnetic (TEM) wave. The TEM feed arms guide the outwardly propagating spherical TEM wave, which is launched at the apex of the TEM feed arms. The reflector converts the spherical wave into an equi-phase aperture. There is an increasing demand for impulse radiating antennas (IRAs) to receive and transmit short pulses. The Impulse Radiating Antenna (IRA) was first conceptualized and eventually designed by Carl Baum in 1989 [1]. Ever since, plenty of papers have filled out the knowledge domain of the IRA [2-4] and innumerous versions of the IRA with different diameters of reflector and various feed arm configurations have been built and tested by Everett Farr and others [4-6]. The objective of this document is to show simulation results in the frequency domain of the electrical characteristics of the IRA modeled using the electromagnetic analysis code CST-MS. This commercial software i.e. with the help of the electromagnetic code, it is possible to analyze electrically large structures on a desktop pc using modest computational resources. In this paper, a CST-MS model which is based on design information provided by E. Farr for an IRA-6 with an 152cm diameter reflector and 45 degree feed arms . However, instead we use the basic 45 degree feed arms and 70 cm diameter reflector configuration. The frequency domain results of the simulation for the reflector IRA is evaluated. The reflector IRA(Fig. 1) consists of a parabolic reflector fed by a self-reciprocal TEM transmission line. The spherical wave that propagates through the TEM feed is converted to the plane wave by the parabolic reflector. Before studying the reflector IRA properties a review of an ideal reflector IRA will be presented.

II. Reflector IRA

Fig.1 shows the typical structure of a reflector-type IRA. It consists of a parabolic reflector and TEM feed arms, which are connected to the reflector through low-frequency matching circuits. The characteristic impedance of the feeding transmission line is chosen to be the same as the characteristic impedance of the TEM feed arms (Z_0). The impedance of each low-frequency matching circuit is chosen to be $Z_0/2$ so that the TEM feed arms are terminated with a matched load at low frequencies. For this design, it is assumed that the feeding transmission line does not disturb the field generated by the antenna.

For the geometry shown in Fig.1, the radiated field on boresight is

$$\overline{E}^{r}(t_r) = \frac{V_0}{r}\frac{\overline{h}_a}{2\pi c f_y}\{\frac{c}{2F}[-u(t_r)+u(t_r-2F/c)]+\delta(t_r-2F/c)\} \quad (1)$$

when the antenna is excited at the apex of the TEM feed arms by an ideal step pulse with amplitude V_0, where c is the speed of light in free space, $t_r = t-r/c$ is the retarded time, h_a is the aperture height, f_g is the geometric

978-1-4244-2120-6/08/$25.00©IEEE.

impedance factor, F is the focal length of the reflector, $u(t)$ is the Heaviside step function, and $\delta(t)$ is the Dirac delta function. Eq. (1) may be re-written for general time dependence:

$$\overline{E}^{r}(t_r) = \frac{\overline{h}_a}{2r\pi c f_y}\{\frac{c}{2F}[-V(t_r)+V(t_r-2F/c)]+\frac{d}{dt}V(t_r-2F/c)\} \quad (2)$$

where $V(t)$ is the voltage applied at the apex of the TEM feed arms. The geometric impedance factor f_g is related to the characteristic impedance of the TEM feed line Z_0:

$$f_g = Z_0/\eta_0; \quad (3)$$

where η_0 is the wave impedance of free space. The aperture height h_a is defined as

$$\overline{h}_a = \frac{f_g}{V_0}\int_{S_a}\overline{E}(\overline{r}')dS' \quad (4)$$

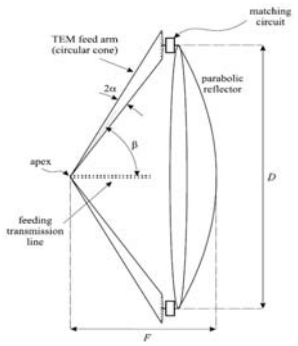

Fig 1
Typical structure of an IRA with a pair of bent circular cones. α is the interior angle of the cone, and β is the angle between the rotational of time axis of the reflector and the axis of the bent circular cone.

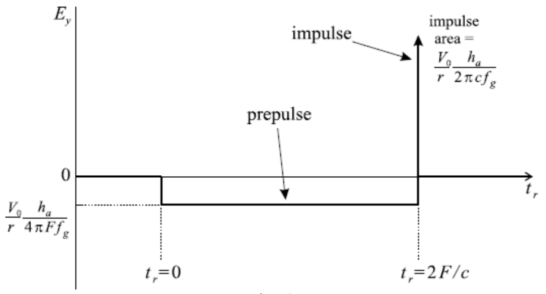

Fig. 2
Radiated field on boresight of a typical reflector-type IRA as a function for a Heaviside step pulse input.
Waveform consists of a prepulse and an impulse.

Which is the integration of the aperture field $\overline{E}(\overline{r}')$ over the aperture S_a when the voltage V_0 is placed across the two TEM feed arms. It is usually assumed that the aperture plane is perpendicular to the rotational axis of the parabolic reflector and passes through the apex of the TEM feed arms. Eq. (1) predicts that for a step excitation, the radiated field on boresight has two parts. These are called the prepulse and the impulse in literature. The step response of a typical IRA is shown in Fig.2. The prepulse is a direct radiation of the TEM feed arms toward the observer. The impulse is the aperture radiation, which is formed by reflection of the spherical TEM wave. There are late-time responses due to multiple internal reflections, which are not predicted by the simple model. The late-time responses are called postpulses and generally not wanted. Three types of geometries are often considered for the TEM feed arms of the reflector-type IRAs: bent circular cones, coplanar conical plates, and curved conical plates. The geometric impedance factors of these types of TEM feed arms are described by simple mathematical expressions, but the expression for the aperture heights can be relatively complicated. The geometry with bent circular cones is shown in Fig 1. The geometric impedance factor of a pair of bent circular cones is

$$f_g = (1/\pi)\cosh^{-1}(\sin\beta/\sin\alpha) \quad (5)$$

where α is the half interior angle of a cone arm, and β is the angle between the rotational axis of a cone arm and the plane of symmetry. When the blockage caused by the TEM feed arms is ignored, the aperture height formed by the TEM feed arms is $D/2$. Thus, the radiated field on boresight becomes

$$\overline{E}^{r}(t_r) = \frac{D}{4rc\cosh^{-1}{}_y(\frac{\sin\beta}{\sin\alpha})}\{\frac{c}{2F}[-V(t_r)+V(t_r-2F/c)]+\frac{d}{dt}V(t_r-2F/c)\} \quad (6)$$

for an input whose time dependence is $V(t)$. The geometry with the coplanar conical plates is shown in Fig.3. It is an appealing geometry because the TEM feed arms do not take space when the geometry is projected onto the aperture plane, and therefore they do not seem to block the aperture in the geometric optics sense, although the TEM feed arms do disturb electromagnetic fields and cause postpulses. The geometric impedance factor of a pair of the coplanar conical plates is

$$f_g = K(m)/K(1-m); \quad m = \tan^2(\beta_1/2)/\tan^2(\beta_2/2) \quad (7)$$

where $K(m)$ is the complete elliptic integral of the first kind, and β_1, β_2 are the angles between the inner and outer edges of a feed arm and the plane of symmetry. The aperture height formed by the TEM feed arms has been calculated as

$$h_a = \frac{\pi m^{-1/4}D}{4K(1-m)}[1-\frac{2}{\pi}\sin^{-1}(\frac{(1-m^{1/2})^2}{1-m})] \quad (8)$$

The first term of Eq. (8) is the aperture height when the blockage due to the TEM feed arms is ignored. The second term of Eq. (8) is the correction for the blockage. Note that the geometry of the IRA with coplanar conical plates has a reflection symmetry. Because the electric fields are zero in the symmetry plane, a second pair of coplanar conical plates can be placed in the symmetry plane without disturbing the fields. The second pair of coplanar conical plates can be either driven independently or connected in parallel to the first pair. The former is useful for transmitting two polarizations. The latter is often preferred because it lowers the input impedance of the IRA by a factor of 2, which makes it easier to match the impedance of the antenna to the source.

978-1-4244-2120-6/08/$25.00©IEEE.

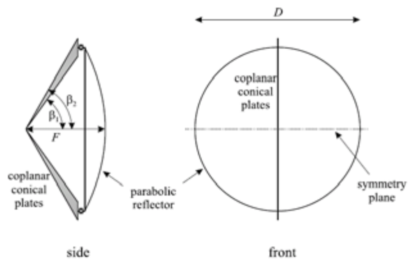

Fig 3

Typical structure of an IRA with a pair of coplanar conical plates. $\beta_1$and β_2 are the angles of the inner and outer edges of the TEM feed arms.

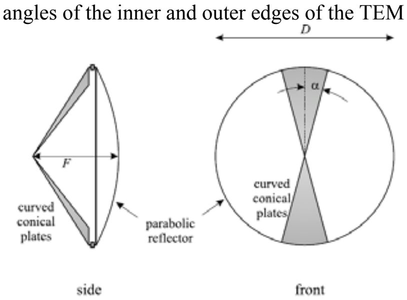

Fig 4

Typical structure of an IRA with a pair of curved plates.
α is the half angle of the fan formed by projection onto the aperture.

The geometry with the curved plates is shown in Fig 4. The geometric impedance factor of a pair of the curved conical plates is

$$f_g = \frac{K(m)}{K(1-m)}, m = [\frac{1-\sin\alpha}{\cos\alpha}]^4 \quad (9)$$

where α is the half angle of the fan that is formed by the projection of the TEM feed arms onto the aperture plane. The aperture height formed by this structure is

$$h_a = \frac{\pi D}{2K(1-m)(1+m^{1/2})} \quad (10)$$

where the aperture blockage caused by the TEM feed arms is not included.

III. FORMULATION OF THE PROBLEM

A. Geometry of the Problem and Approach to Solution

The geometry of the problem is shown in Fig. 3, where the IRA structure consists of a 60cm diameter paraboloidal reflector and four feed arms with 45 degree spacing. This fig. shows the front and side views of the IRA to be modeled in CST-MS. Let us consider this IRA as shown, which has two pairs of conical-coplanar plate TEM feed arms, which are placed perpendicular to each other. The TEM feed arms have a conical geometry within a sphere of radius centered at the drive point, where a spherical TEM wave launched at the drive point propagates outwardly without disturbance. The angles associated with the TEM feed arms are chosen such that the characteristic impedance of each pair of the arms is 400Ω in the undisturbed section. Outside the spherical region of radius, the TEM feed arms are linearly tapered and connected to the reflector through 200Ω chip resistors, which are used as low frequency matching circuits. The IRA is excited at the drive point(focal point). Each pair of arms is excited independently to radiate two polarizations or can be excited in parallel to lower the characteristic impedance of the arm structure. In this paper, the arms in the positive-*y* half-space are connected together, and the arms in the negative-*y* half-space are connected together at the drive point. The resulting characteristic impedance of the TEM feed structure is 200Ω. The IRA has redundancies in the geometry. By eliminating these redundancies, the efficiency of the model can be significantly improved on carrying out the numerical analysis of the IRA. Note that one pair of TEM feed arms is placed in the symmetry plane of the other pair of TEM feed arms, where the tangential electric field is zero. Thus, the field generated by the first pair is independent of the existence of the second pair, and the fields generated by the two pairs are simply the orthogonal versions of each other. Thus, the geometry of the IRA with one pair of TEM feed arms can produce enough data to predict the response of the IRA with two pairs of TEM feed arms. The 2-arm IRA still has reflection symmetry. This allows one to replace half of the 2-arm IRA geometry with a perfect electric conductor (PEC) plane placed orthogonal to the TEM feed arms. The PEC plane mirrors the remaining geometry. Thus, only half of the reflector and one TEM feed arm need are required in the numerical model. Here, CST-MS software generates the mesh for the simulated model which consists of the paraboloidal reflector, the feed arms and the drive point which is modeled using a simultaneous voltage source. The chip resistor is modeled using a 200Ω lumped impedance model. The plates which make up the feed arms are automatically discretized by CST-MS into appropriate meshing for a maximum frequency of 7GHz. The dimensions are summarized as $\beta_0 = 73.74^o$, $\beta_1 = 65.03^o$ and $\beta_2 = 82.85^o$ for the IRA.

B. Analysis of the Impulse-Radiating Antenna

The analysis of this simulated IRA in terms of its radiated field along its optical axis was performed, and the simulated results are shown from fig. 5 to fig.11. The details of the mathematical analysis of this antenna are not presented here. It is noted that the radiated field ,assumes an ideal Gaussian function source. After a time interval of (where is the focal length of the reflector), the radiation from the reflector antenna is seen, and it is a time derivative of the input step function. This corresponds to the impulse function in fig. 8, with a certain area. The area under the impulse is equal to the area under the prepulse or feed step. The postpulse consists of the diffracted signals from the launcher plates (the TEM feed lines) and the circular rim of the reflector. It is interesting to note that these diffraction terms have a canceling effect, since they are of opposite signs, in the time domain. The net area of prepulse and impulse is zero, and the net area of the postpulse is also zero. As required, the net area of the entire radiated field is zero, resulting in no dc radiation. An extensive set of far-field simulations were performed, and a representative waveform at a distance of 100 m is shown along with the azimuthal variation of the peak electric field in Fig. 10.

IV. RESULTS

Here, we have considered a reflector Impulse Radiating Antenna with f/d ratio as 0.333,where the focal length is 20cm and the diameter of the reflector is 60 cm. The feed arms are the conical co-planar transmission line

978-1-4244-2120-6/08/$25.00©IEEE.

for the launching of the TEM spherical wave on to the paraboloidal reflector, is placed at some point away from the focus. This offset is a variable quantity and can be changed accordingly for optimum results. The offset is made for the reason that the feed arms are to be fed simultaneously at any instant. Coaxial feed is used to excite the antenna i.e. the conical, coplanar feed arm transmission line. The characteristic impedance of the coaxial cable is 100 ohms. The center conductor of the feed coaxial cable is connected to one of the feed arm and the outer connecter is connected to the ground plane, whereas for the other feed coaxial cable, the center conductor is connected to the ground plane and the outer conductor is connected to the other feed arm. The distance between the center conductor-ground plane and center conductor -feed arm is optimized for the best possible results and minimum flash over. The point of the feed is also the area of minimum current distribution ,thereby feeding a balanced antenna with a unbalanced feed. The resistive load consists of 200 ohm resistors connected at the other end of the feed arms and the paraboloidal reflector. This termination influences the low frequency radiation by giving both electric and magnetic dipole moments which gives a radiation pattern peaking in roughly the same direction as the high-frequency reflector pattern. The structure used in this design is shown in Fig. 5(a,b).

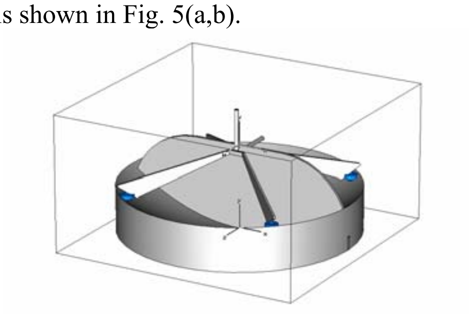

Fig. 5a
Perspective view of an paraboloidal reflector IRA with a pair of coplanar plates

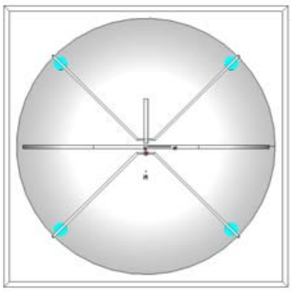

Fig. 5b
Top view of the paraboloidal reflector IRA with a pair of coplanar plates

The dB reflection coefficient vs. frequency, which is proportional to the received field, is plotted in fig.6, which shows a satisfactory ultra bandwidth of around 6 GHz. Fig.7 shows the dB directivity vs. frequency , which agrees well with the shape and peak gain found in the measurements documented the IRA's. fig 8. Shows the reflected waveform in time domain from the IRA at a probe placed 100m at the boresight. The corresponding VSWR for this antenna for the frequency range of 200 MHz to 7 GHz can be seen from the fig 9. The measured E-plane far-field pattern for this antenna, excited at 2.55 GHz is shown in fig 10 ,this E_{θ} radiation vs. frequency for the IRA as a transmitter with simultaneous feed located at the focal point of the reflector, where the four feed arms meet. This fig shows the antenna with a symmetric far-field pattern. It was found that the antenna has a -10 dB or lower response for a bandwidth from 250 MHz to 7 GHz. The response on the Smith chart can be seen in the fig.11.

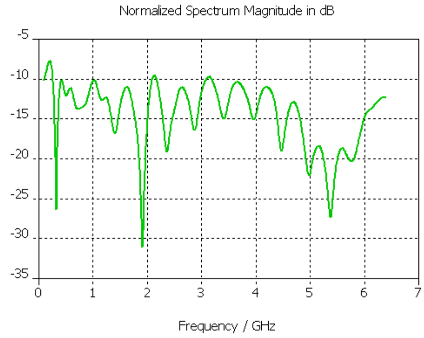

Fig. 6
dB reflection coefficient vs. frequency

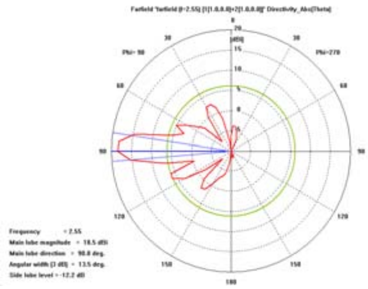

Fig. 7
dB directivity vs. frequency at a freq of 2.55 GHz.

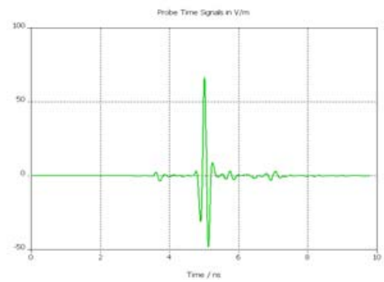

Fig 8
Reflected waveform in time domain from the IRA at a probe

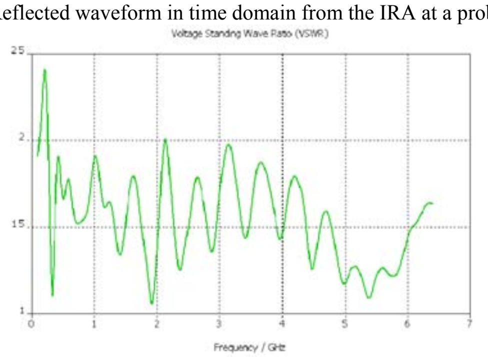

Fig 9
VSWR of the reflector IRA.

978-1-4244-2120-6/08/$25.00©IEEE.

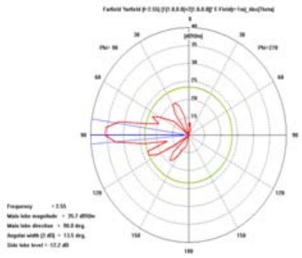

Fig 10
E-field of the reflector IRA at a distance of 1m at freq of 2.55 GHZ

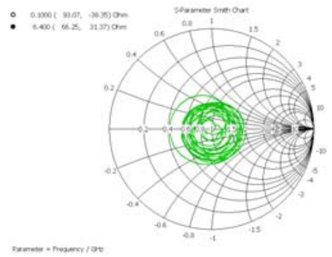

Fig 11
. Smith chart of the reflector IRA .

CONCLUSIONS

An UWB Impulse Radiating antenna is designed and simulated in CST-MS for frequency range in 250 MHz to 7 GHz range. The feed and the Impulse Radiating antenna were simulated for various characteristics like frequency domain reflections, VSWR, insertion loss, radiation pattern and gain etc. The half power beamwidth and antenna factor of the antenna were also calculated. The antenna is wideband, non dispersive, directive and has low VSWR. The non dispersive and ultra wideband characteristics make this antenna suitable for many other applications were the main requirement is pulse optimised wideband antenna. Therefore this antenna can be used in applications of pulse RADAR in collision avoidance, docking, and detection of objects buried in lossy materials (e.g. mine detection), detection of stealth targets and WB receptions required in electronic intelligence (ELINT) and electronic warfare (EW). In addition such antenna is useful in satellite communications were space & weight are conserved by supporting many communication channels with only one antenna. This WB antenna can also be considered for replacement of a large set of narrowband antennas in RCS range for wideband RCS measurements.

REFERENCES

[1] C. E. Baum, “Radiation of Impulse-Like Transient Fields”, Sensor and Simulation Note 321, November 1989.

[2] C. E. Baum, E. G. Farr and D. V. Giri, “Review of Impulse-Radiating Antennas”, Chapter 12 in *Review of Radio Science 1996-1999*, W. S. Stone, ed., Oxford University Press, 1999.

[3] K. Kim and W. R. Scott, Jr., “Numerical Analysis of the Impulse-Radiating Antenna”, Sensor and Simulation Note 474, June 2003.

[4] L. H. Bowen, E. G. Farr, C. E. Baum, T. C. Tran and W. D. Prather, “Results of Optimization Experiments on a Solid Reflector IRA”, Sensor and Simulation Note 463, January 2002.

[5] E. Farr, “Experimental Validation of IRA Models”, Sensor and Simulation Note 364, January 1994.

[6] E. Farr, “Analysis of the Impulse Radiating Antenna”, Sensor and Simulation Note329, July 1991.

[7] Majid Manteghi and Yahya Rahmat-Samii, "A Novel UWB Feeding Mechanism for theTEM Horn Antenna, Reflector IRA, and the Vivaldi antenna", *lEEE Antennas and propagation Magazine,* Vol. 46, No. 5, October 2004.

[8] C. E. Baum [1991], “Configurations of TEM Feed for an IRA,” *Sensor and Simulation Note* 327.

[9] C. E. Baum [1997], “Some Topics Concerning Feed Arms of Reflector IRAs,” *Sensor and Simulation Note* 414.

[10] C. E. Baum [1995], “Variations on the Impulse-Radiating-Antenna Theme,” *Sensor and Simulation Note* 378.

[11] L. H. Bowen and E. G. Farr [1998], “E-Field measurements for a 1 Meter Diameter Half IRA,” *Sensor and Simulation Note* 419.

[12] H.-T. Chou, P. H. Pathak, and P. R. Rousseau [1997], “Analytical Solution for Early-Time Transient Radiation from Pulse-Excited Parabolic Reflector Antennas,” *IEEE Trans. Antennas and Propagation*, pp. 829–836.

[13] E. G. Farr [1993], “Optimizing the Feed Impedance of Impulse Radiating Antennas, Part I Reflector IRAs,” *Sensor and Simulation Note* 354.

[14] E. G. Farr and C. E. Baum [1993], “The Radiation Pattern of Reflector IRA: Early-Time Response,” *Sensor and Simulation Note* 358.

[15] E. G. Farr and G. D. Sower [1995], “Design Principles of Half Impulse Radiating Antennas,” *Sensor and Simulation note* 390.

[16] D. V. Giri [1995], “Radiated Spectra of Impulse Radiating Antennas (IRAs),” *Sensor and Simulation Note* 386.

[17] D. V. Giri and C. E. Baum [1994], “Reflector IRA Design and Boresight Temporal Waveforms,” *Sensor and Simulation Note* 365.

[18] D. V. Giri et al [1995], “A Reflector Antenna for Radiating Impulse-Like Waveforms,” *Sensor and Simulation Note* 382.

[19] D. V. Giri et al [1997], “Design, Fabrication, and Testing of a Paraboloidal Reflector Antenna and Pulser System for Impulse-Like Waveforms,” *IEEE Trans. Plasma Science*, pp. 318–326.

[20] Y. Rahmat-Samii [1992], “Analysis of Blockage Effects on TEM-Fed Paraboloidal Reflector Antennas,” *Sensor and Simulation Note* 347.

[21] Y. Rahmat-Samii and D. V. Giri [1992], “Analysis of Blockage Effects on TEM-Fed Paraboloidal Antennas (Part II: TEM Horn Illumination),” *Sensor and Simulation Note* 349.

[22] Kangwook Kim, “Numerical and Experimental Investigation of Impulse-Radiating Antennas for Use in Sensing Applications” , School of Electrical and Computer Engineering Georgia Institute of Technology April 2003.